1. FIRING PHENOMENA

1.1 Introduction

Ceramic bodies undergo upon firing one or more of a series of operations and processes. These usually lead to an increase in their bulk density, a process known as **densification**. The main changes occurring on firing are:

1. Sintering
2. Grain growth
3. Vitrification
4. Solid state reactions
5. Allotropic transitions

1.2 Sintering

Compacted ceramic powders undergo several significant changes during heat treatment, including but not limited to chemical reactions via decomposition and/or oxidation, phase transformations and sintering.

Sintering is a phenomenon whereby compacted powders will bond when heated to temperatures above half their melting temperature.

The goal of the sintering process is to convert highly porous compacted powder into high strength bodies. During sintering, the significant strengthening of the ceramic body is due to the formation of inter-particle bonds resulting from atomic motion at the sintering temperature.

1.2.1 Sintering stages

Sintering is driven by particle diffusion that leads to a reduction in surface energy. This can occur by two possible paths, as shown in Figure (1.1). The first path is through coarsening of the ceramic leading to an increase in the average particle size. The second path is via the elimination of solid-vapor interfaces and the creation of grain boundaries, followed by grain growth that leads to densification. In the second path, the shrinkage of the compacted body must occur. These two paths are usually competitive. If coarsening dominates, the sizes of the pores and grains of the body increase with time. If densification dominates, the pore sizes decrease and pores eventually disappear and the entire body shrinks.

There are two common types of sintering: solid-state and liquid-phase sintering. Solid-state sintering is a process that converts compacted powders to strong, dense ceramic bodies upon heating. Liquid-phase sintering on the other hand, is a process accompanied by the presence of co-existing liquid phases of liquid and solids. Liquid-phase sintering is commonly used for materials which are hard to sinter and have wide applicability in industrial processes.

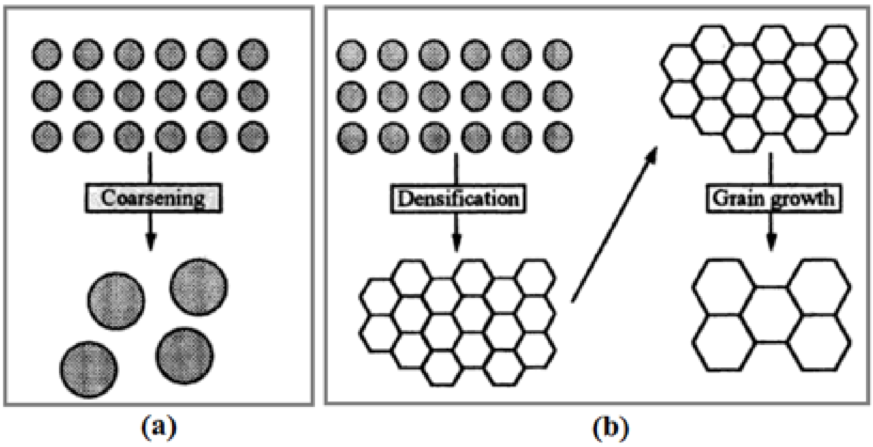

Fig (1.1) Schematic of the paths for surface energy reduction in sintering. Path 1 is a) coarsening where small particles combine to form larger-sized particles and 2 is b) the densification of particles followed by grain growth.

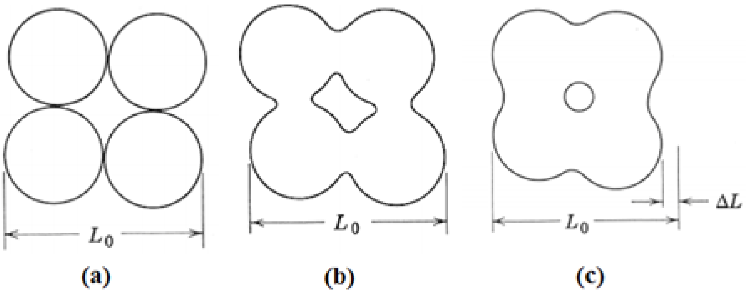

Fig (1.2) Schematic representation of the neck formation during solid-sintering due to (a) powder compaction, (b) neck growth, and (c) neck growth accompanied by densification

The reduction in surface energy can be used to explain the three main stages of solid-state sintering, as are shown in Figure (1.2). In the first stage, atoms migrate towards the points of contact between particles to form necks as this filling process reduces the surface area and the surface energy. In the second stage, the grain boundaries grow because, as atoms are removed from the grain boundary and diffuse towards the neck, this causes the centers of particles to mutually converge. In the final stage, the pore is slowly eliminated as grain boundaries merge.

In liquid-phase sintering, the liquid phase can be initiated via two common techniques. In the first method, powders of different chemistries are mixed so that the interaction of the powders results in the formation of a liquid during sintering. The liquid formation in this method can be a result of the melting of one component of the formation of a eutectic phase. In the second method, the liquid can be formed by heating a powder to a temperature between the liquidus and solidus temperatures, resulting in co-existing liquid and solid phases.

Liquid-phase sintering can also be described by three phases that are driven by surface energy reduction. In the first stage, capillary action pulls the liquid into pores so that the liquid wets the solids. In the second stage, smaller particles in the solids go into solution, they preferentially precipitating on larger particles, leading to densification. In the final stage, a solid skeletal network forms and the liquid moves into pores so that the wetting liquid reduces the porosity and interfacial energy of the solid phase, leading to additional densification.

1.2.2 Solid state sintering mechanisms

There are basically 5 atomic sintering mechanisms by which mass can be transferred in a powder compact:

- Evaporation – condensation mechanism
- Surface diffusion
- Bulk (or volume diffusion)
- Grain boundary diffusion
- Viscous flow

(a) Evaporation – condensation mechanism

In this mechanism, solid atoms are transferred to the gas phase from areas of high convexity to areas of lower convexity, typically the neck area between the particles. The driving force for such mass transport is the pressure difference between surface and neck area. (Figure 1.3)

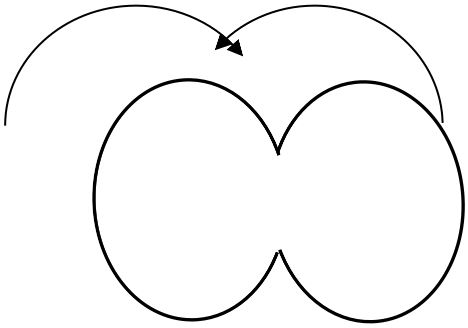

Fig (1.3) Path of mass transport in Evaporation – condensation sintering

During the initial stage of sintering, it has been proved that the linear shrinkage associated with such mechanism is related to the time of sintering (t) and particle size (D_p) by the following equation:

$$\frac{\Delta L}{L_0} = K.\frac{t^{2/3}}{D_p^{4/3}} \qquad (1.1)$$

Here, K is a constant depending on the sintering temperature, the interfacial tension between vapor and solid phase and the vapor pressure of the gas phase. This mechanism is only exhibited by solids displaying high vapor pressure at elevated temperatures such as alkali chlorides.

(b) Bulk diffusion mechanism

It is assumed in this mechanism that the material diffuses away from the grain boundary area through the bulk. This diffusion proceeds essentially through vacancies present in the bulk. The equation relating the relative shrinkage to time and particle size during the initial stage of sintering stands as follows:

$$\frac{\Delta L}{L_0} = K.\frac{t^{1/2}}{D_p^{3/2}} \qquad (1.2)$$

This mechanism requires a lot of energy since the motion of ions (or atoms) across the bulk requires a high concentration of vacancies which can only be achieved at elevated temperature.

(c) Grain boundary diffusion mechanism

This is a more favorable mechanism than the previous. It assumes the motion of atomic species along the grain boundaries until reaching the neck region between the particles. (Figure 1.4)

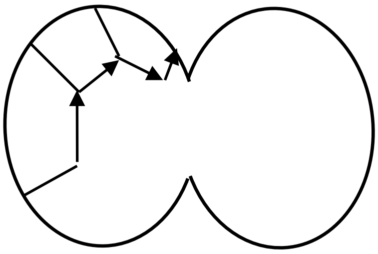

Fig (1.4) Path of mass transport in Grain Boundary sintering

The equation relating the relative shrinkage to time and particle size during the initial stage of sintering stands as follows:

$$\frac{\Delta L}{L_0} = K.\frac{t^{1/3}}{D_p^{4/3}} \qquad (1.3)$$

(d) Surface diffusion mechanism

In this model the atoms (or ions) are assumed to diffuse along the surface from an area that is near the neck region to the neck area. The appropriate expression for the relative linear shrinkage with time and particle size in the initial sintering period takes the following form:

$$\frac{\Delta L}{L_0} = K.\frac{t^{2/5}}{D_p^{8/5}} \qquad (1.4)$$

This model is by far more likely than the two previous ones since it is energetically more favorable. It is responsible for the rounding off edges of ceramic bodies on firing.

(e) Viscous sintering

This model is rather confined to sintering glass particles. It involves the motion of particles rather than atoms owing to a lowering of viscosity at high temperature. The remarkable feature is that the relative linear shrinkage does not depend on particle size and is linearly dependent on time as follows:

$$\frac{\Delta L}{L_0} = K.t \tag{1.5}$$

(1.2.4) Sintering kinetics

The general form of the dependence of linear shrinkage on time t and particle size D_p takes the form:

$$\frac{\Delta L}{L_0} = K.\frac{t^n}{D_p^m} \tag{1.6}$$

For a fixed value of D_p and m, this simplifies to:

$$\frac{\Delta L}{L_0} = c.t^n \tag{1.7}$$

The values of the constants n and m depend on the sintering mechanism and are summarized in the following table.

Table 1: Values of the constants m and n in Equation (1.6)

Mechanism	Evap. – Cond.	Bulk Diff.	G.B. Diff.	Surf. Diff.	Viscous
m	$4/3$	$3/2$	$4/3$	$8/5$	0
n	$2/3$	$1/2$	$1/3$	$2/5$	1

Differentiating of the LHS of equation (1.7) with respect to time does not result in a convenient expression for the rate of sintering since this latter is a three – dimensional phenomenon. If sintering is assumed to take place at equal rate in all three directions, then we consider a cube of edge length L_0, which will shrink after time t to L.

Since $V = L^3$, then $dV = 3L^2dL$.

$$\frac{dV}{V} = \frac{3L^2dL}{L^3} \rightarrow \frac{dV}{V} = \frac{3dL}{L}$$

If the values of L and V do not change appreciably during sintering, we may write:

$$\frac{\Delta V}{V_0} = \frac{3\Delta L}{L_0} = 3c.t^n \qquad \text{or} \qquad V = V_0[1 - 3c.t^n]$$

The rate of sintering is then defined as $\frac{dV}{dt}$, which yields the equation:

$$\frac{dV}{dt} = - \; 3V_0.c.n.t^{n-1} \tag{1.8}$$

The negative sign implies that the rate of sintering decreases with time.

The coefficient of t^{n-1} in the above equation represents the reaction rate constant k, so that:

$$k = 3V_0.c.n \tag{1.9}$$

The value of the reaction rate k in equation (1.9) is related to temperature through an Arrhenius type equation:

$$k = Ae^{-\frac{E}{RT}} \tag{1.10}$$

Where: E = Activation energy for sintering (J.mol^{-1}) and R, the general gas constant = 8.314 J.mol^{-1}.K^{-1})

One may write from Equations (1.9) and (1.10):

$$c = c_0 e^{-\frac{E}{RT}} \tag{1.11}$$

Where: $c_0 = \dfrac{A}{3nV_0}$

To obtain the activation energy, the value of c is obtained at each temperature, by re-writing (1.7) in the form:

$$\ln \frac{\Delta L}{L_0} = \ln c + n.\ln t \tag{1.12}$$

Plots of the LHS against $\ln t$ are then performed at each sintering temperature T to obtain the values of c and n.

The value of n discloses the sintering mechanism, as per Table 1, while the values of c at different temperatures are used to obtain the activation energy E as follows: Equation (1.11) is rewritten in the form:

$$\ln c = \ln c_0 - \frac{E}{RT} \tag{1.13}$$

A plot of $\ln c$ against $1/T$ produces a straight line of slope = $-\dfrac{E}{R}$

Usually the activation energies for surface, grain boundary and bulk diffusion increase in that order. Thus, surface diffusion is more favored at low temperatures while grain boundary and bulk diffusion at higher temperatures. Table 1 shows that the dependence on shrinkage on particle size is highest in surface diffusion. This means that fine grinding will enhance that mechanism. As for viscous sintering it does not depend on particle size as previously stated.

Also, the previous remarks hold for intermediate and final sintering stages although the equations are not identical to those deduced for the initial stage.

1.2.4 Densification curves

The progress of sintering can be followed by determining the percent linear shrinkage occurring with time at fixed temperature. Curves drawn at different temperatures are called densification curves. They show that the linear shrinkage tends to reach some asymptotic value after enough time has elapsed. In practice, however, the percent densification is usually plotted rather than linear shrinkage. This is defined as follows:

$$\%Dens. = \frac{\rho_B}{\rho_p} \times 100\% = (1-\varepsilon) \times 100\% \tag{1.14}$$

Where: ρ_p is the true particle density, ρ_B is the bulk density and ε the porosity.

The percent densification can be used to predict the percent linear shrinkage, assuming that shrinkage is isotropic in all directions, in the following way:

Consider a cubic body, and let the initial length of specimen before firing = L_0 and the length at any time during firing = L.
Hence the original mass of body = $L_0^3.\rho_0$
Where: ρ_0 is the initial bulk density.
The mass at any time = $L^3.\rho$
Since the mass is constant, then:

$$L_0^3.\rho_0 = L^3.\rho$$

Since the percent shrinkage = $\frac{L_0 - L}{L_0}$, we then get:

$$\frac{\Delta L}{L_0} = 1 - \left(\frac{\rho_0}{\rho}\right)^{\frac{1}{3}} \qquad (1.15)$$

In practice it is common to deduce the linear shrinkage from density measurements.
Figure (1.5) shows the general shape of densification curves.

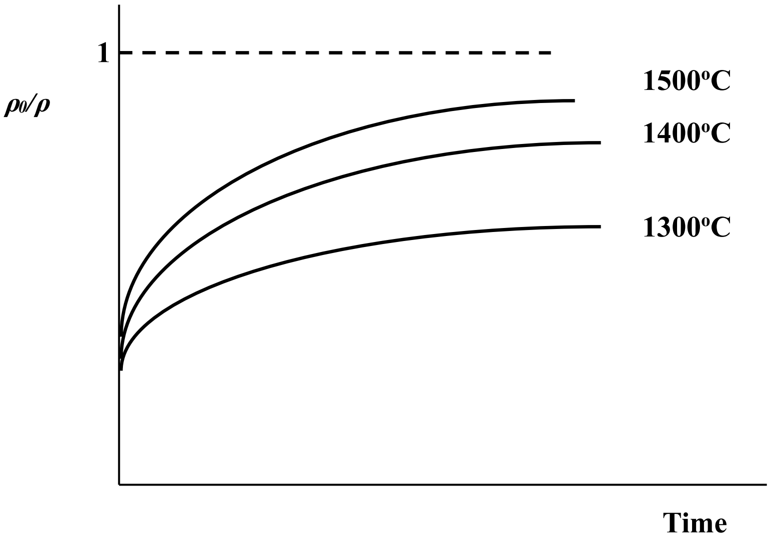

Fig (1.5) Densification curves

An approximate form of Equation (1.15) can be obtained by rewriting this latter in the form:

$$\frac{\Delta L}{L_0} = 1 - \left(1 - \frac{\rho - \rho_0}{\rho}\right)^{\frac{1}{3}}$$

Since $\frac{\rho - \rho_0}{\rho}$ is usually very small, we can use the approximation:

$$\left(1 - \frac{\rho - \rho_0}{\rho}\right)^{\frac{1}{3}} \approx 1 - \frac{1}{3}\left(\frac{\rho - \rho_0}{\rho}\right)$$

So that Equation (1.16) can be rewritten as:

$$\frac{\Delta L}{L_0} = 1 - \left[1 - \frac{1}{3}\left(\frac{\rho - \rho_0}{\rho}\right)\right] \approx \frac{1}{3}\left(1 - \frac{\rho_0}{\rho}\right) \qquad (1.16)$$

For example, let us assume that $\rho_0 = 4.18$ g.cm^{-3}, and that $\rho = 4.3$ g.cm^{-3}

Applying equation (1.15), we get: $\frac{\Delta L}{L_0}$ = 0.09389, whereas from Equation (3.16): $\frac{\Delta L}{L_0}$ = 0.09302, the error is less than 1%.

1.3 Grain growth

1.3.1 Theory

During firing, there occurs a coarsening of grain. The reason behind this behavior can be understood from the following discussion. Consider Fig. (1.6) which shows a boundary between two grains, the atoms of which being in different plane sets. It can be proved that atoms on the concave side of the boundary have a higher energy than those on the convex side. So that, as their mobility increases on raising temperature, these high energy atoms will jump across the boundary to the lower energy convex region and the boundary will move **towards its center of curvature** (dashed position in figure).

Consider now the point of intersection of three grain boundaries in a one phase material. The interfacial tension forces holding the grain together are therefore equal. So, for equilibrium to occur at this point, the angles between these forces must be equal = 120°. This is the case in six sided grains.

Hence such grain will have fixed linear boundaries. Such grains will neither grow nor shrink. If a grain has its number of sides < 6, then in order that the angles between the boundaries be equal to 120°, the boundaries must be curved outwards. This means that these boundaries will move inwards and such grains will shrink and given enough time, will ultimately disappear. Conversely, grains with sides > 6 will have convex boundaries and will tend to grow on the expense on their neighbors which have less than 6 sides. See Fig. (1.7)

The speed at which grains grow is governed by the equation:

$$\frac{dD}{dt} = \frac{k}{D}$$

Integrating, we get:

$$D^2 = D_0^2 + 2kt \qquad (1.17)$$

Where: D_0 is the average grain size at zero time.

1.3.2 Grain growth inhibition

It has been seen earlier that large grains are associated with lower mechanical properties. Another important reason why excessive grain growth should be prevented has to do with the elimination of porosity on firing. Pores are usually eliminated by diffusing towards the grain boundaries.

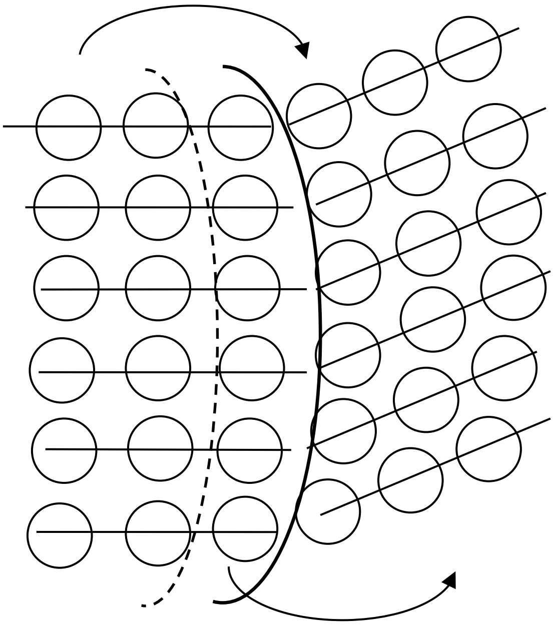

Fig (1.6) Atomic representation of a grain boundary

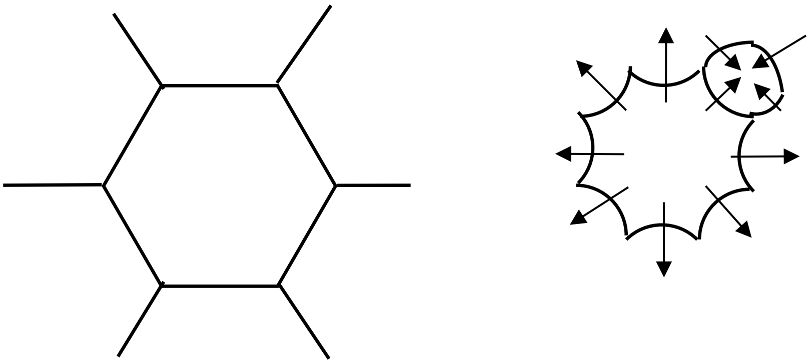

(a) Stable non-moving boundaries (b) Grain growth if n > 6

Fig (1.7) Boundary motion causing grain growth or shrinkage

As they reach these boundaries, they tend to move along them to the external surface where they ultimately disappear. Therefore, the extent to which the elimination of pores proceeds will depend on their reaching the boundaries during the available firing time. If the grains are too large, then pores will have to move a longer distance across the grain, and it may not be possible for them to reach its boundaries during the available firing time. This will result in remnant porosity in the fired body that will negatively affect its mechanical properties.

Prohibiting grain growth is done by adding, in small amounts, a foreign material the atoms of which can easily diffuse to align themselves along boundaries.

These will exert a drag force on this boundary and reduce its mobility. For example, adding strontium zirconate to alumina can stop grain growth to an appreciable extent.

To conclude this section, it is worth mentioning that in some rare instances, grain growth is encouraged despite its negative impact on mechanical properties. A typical such instance occurs on firing magnesite or dolomite refractories. These products can slowly react with atmospheric water vapor and carbon dioxide. When their grains are left to coarsen on firing, their reduced surface area will decrease this effect.

1.4 Vitrification

This is the formation of a viscous liquid phase at high temperature due to partial melting. It is sometimes a major process in smoothing the surface and imparting reasonable strength, as in firing of porcelain and some refractory products. The formed liquid flows into the available pores. By surface tension, it will pull the particles together causing more shrinkage. Also, sintering can occur as mass transfer can occur from the convex parts of the particles, by diffusion through the melt, to be precipitated along the concave region between particles. Too much vitrification is undesirable, as flow under gravity may take place, causing **warping**.

Solved examples

Example 1.1

The following data relates to the change in length of an alumina disk upon firing at 1300°C. Determine the prevailing sintering mechanism during the initial sintering period.

Time h	0	1	2	4	8	12	20	30
Length mm	12	11.3	11.1	10.9	10.6	10.5	10.3	10.25

Estimate the time after which the initial stage terminates.

Solution

Since in general $\frac{\Delta L}{L_0} = K.t^n$, then if logarithms are taken to both sides:

$\log \frac{\Delta L}{L_0} = \log K + n.\log t$

Hence a plot of $\log \frac{\Delta L}{L_0}$ against $\log t$ should produce a straight line of slope = n. determination of that parameter will help specifying the mechanism prevailing during the initial stage of sintering.

Fig (1.8) shows the results obtained. It appears that the curve stops being linear after about 8 hours, which is the approximate period in which initial sintering prevails. **The calculated slope of line = 0.33**, suggesting a grain boundary diffusion mechanism.

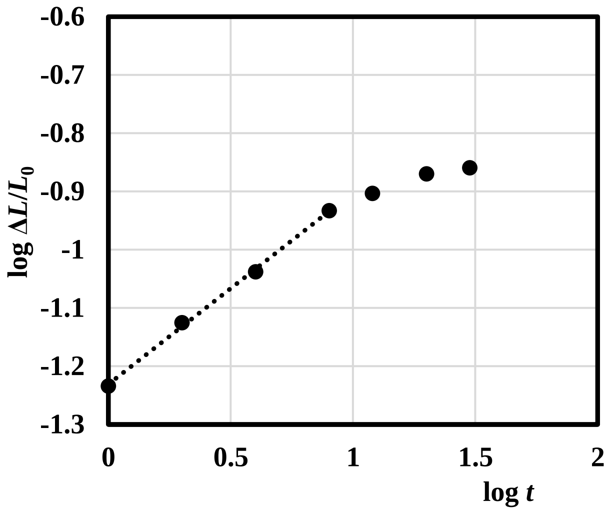

Fig (1.8) Plot of log $\frac{\Delta L}{L_0}$ against log t

Example 1.2

It is known that solid state sintering of a certain ceramic powder in its early stages is controlled by grain boundary diffusion. A cylindrical compact is prepared out of 150 μm particles and sintered at 1400°C for 2 hours. The percent linear shrinkage = 4.8%. Evaluate the corresponding linear shrinkage that would occur if the particle size was decreased to 75 μm and the sintering time increased to three hours.

Solution

For grain boundary diffusion: $\frac{\Delta L}{L_0} = K.\frac{t^{1/3}}{D_p^{4/3}}$

Hence: $0.048 = K.\frac{2^{1/3}}{150_p^{4/3}}$ and $K = 30.3$

At $t = 3$ and $D = 75$ we get: $\frac{\Delta L}{L_0}$ = **0.138**

Example 1.3

The following data show the variation of bulk density with time of an alumina pressed cylinder as sintered at 1400°C: From these data, indicate the probable mechanism for diffusion in the initial stage of sintering.

Time min.	0	30	60	90	120	150	300
ρ g./cm^3	2.9	3.2	3.28	3.33	3.4	3.44	3.6

Solution

The following table shows the calculations:

Time min.	0	30	60	90	120	150	300
ρ **g./cm^3**	2.9	3.2	3.28	3.33	3.4	3.44	3.6
ρ_0/ρ	1	0.9063	0.8841	0.8709	0.8529	0.843	0.8056
$\Delta L/L_0$	0	0.0323	0.0402	0.045	0.0516	0.0553	0.0695
log t		1.4771	1.7782	1.9542	2.0792	2.1761	2.4771
log $\Delta L/L_0$		-1.491	-1.396	-1.346	-1.287	-1.257	-1.158

The plot in Fig (1.9) yields a slope = 0.35 suggesting grain boundary diffusion

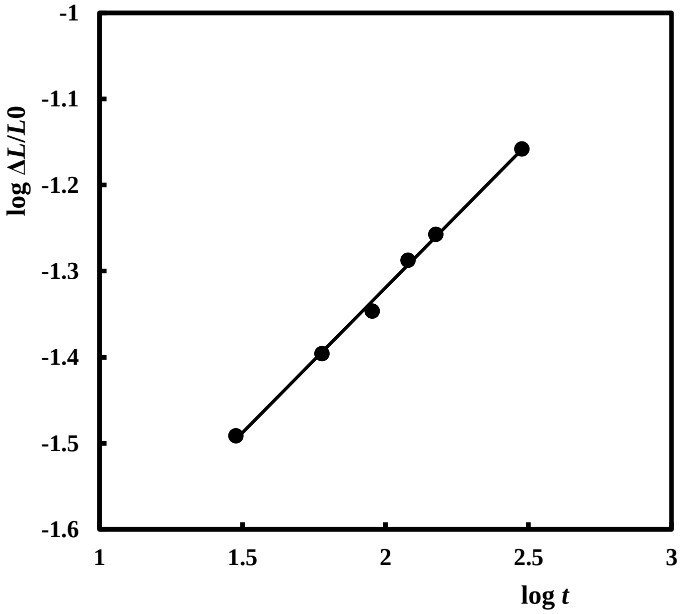

Fig (1.9) Plot of log $\frac{\Delta L}{L_0}$ against log t

Example 1.4

The following values of average grain size were recorded on firing magnesia compacts at 1500°C.

Time h	1	2	3	4	5	6
***D* µm**	240	250	263	275	288	300

Represent these data on a linear plot and deduce the average initial grain size

Solution

A plot of D^2 against time is shown in Fig (1.10)

The intercept is at about D^2 = 50000, corresponding to an average initial grain size = **224 µm.**

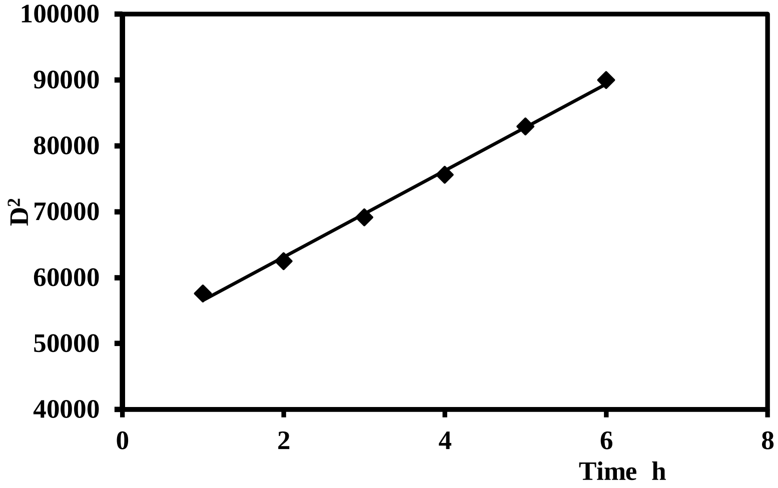

Fig (1.10) Plot of D^2 against t

Example 5

Barium hexa-ferrite powder ($BaO.6Fe_2O_3$) was pressed into cylindrical pellets at 120MPa. The following data were obtained for the pellet density (g.cm^{-3}) through the initial sintering stage of the pressed pellets at four different temperatures. Deduce the sintering mechanism and determine the activation energy for the initial sintering stage. (Ba = 137, Fe = 56)

Time h	**0**	**0.4**	**1**	**1.5**	**2**	**2.5**	**3.5**	**5**
1150	4.58	4.67	4.69	4.73	4.77	4.80	4.84	4.88
1200	4.58	4.69	4.77	4.80	4.85	4.87	4.93	5.01
1250	4.58	4.70	4.80	4.85	4.89	4.94	5.00	5.07
1300	4.58	4.74	4.83	4.89	4.94	4.98	5.06	5.15

Solution:

To obtain the sintering mechanism, $\Delta L/L_0$ is calculated from equation (1.15) with $\rho_0 = 4.58$ g.cm^{-3}

Time h	**0**	**0.4**	**1**	**1.5**	**2**	**2.5**	**3.5**	**5**
1150	0.0000	0.0065	0.0079	0.0107	0.0134	0.0155	0.0182	0.0209
1200	0.0000	0.0079	0.0134	0.0155	0.0189	0.0202	0.0242	0.0294
1250	0.0000	0.0086	0.0155	0.0189	0.0216	0.0249	0.0288	0.0333
1300	0.0000	0.0114	0.0175	0.0216	0.0249	0.0275	0.0326	0.0383

Power curves are fitted through the $\Delta L/L_0 - t$ curves to obtain the equations shown in Figure (1.11). The average value of the four exponents = 0.51, suggesting a **bulk diffusion mechanism.**

To obtain the value of activation energy of sintering, the following steps are carried out:

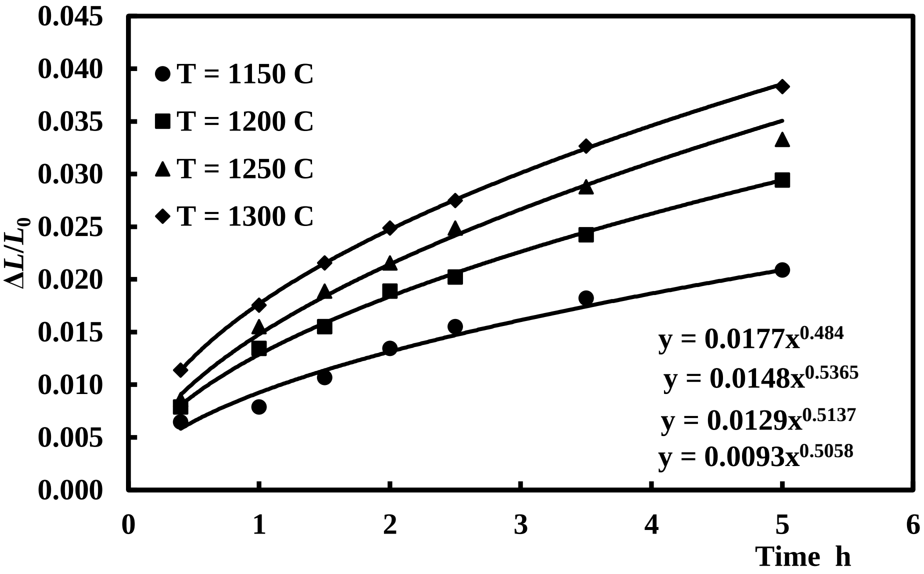

Fig (1.11) Sintering curves of barium hexaferrite

The values of the constant c to be used in equation (1.11) are obtained from the figure as shown in table. Values of $\frac{1}{T}$ and $\ln c$ are also reported.

T °C	1150	1200	1250	1300
c	0.00928	0.01287	0.0148	0.0177
$1/T$ K^{-1}	0.0007	0.00068	0.00066	0.00064
$\ln c$	-4.6777	-4.3505	-4.2131	-4.0342

A fitted straight line between the entries of the last two rows produces a slope = -9336 From which the value of activation energy of sintering is calculated as: $\boldsymbol{E = 77621\ \mathrm{J.mol^{-1}}}$

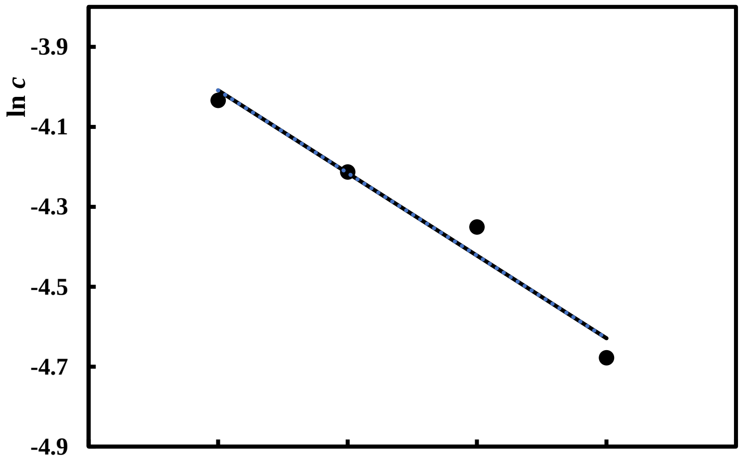

Fig (1.12) Determination of activation energy of sintering